Solid Earth Discuss., 5, 811–839, 2013
www.solid-earth-discuss.net/5/811/2013/
doi:10.5194/sed-5-811-2013

Solid Earth
Discussions
Open Access

Short-lived tectonic switch mechanism for long-term pulses of volcanic activity after mega-thrust earthquakes

M. Lupi[1,*] **and S. A. Miller**[1]

[1]Steinmann Institue, Geodynamics/Geophysics, University of Bonn, Bonn, Germany
[*]now at: ETH Zurich, Department of Earth Sciences, Zurich, Switzerland

Received: 23 May 2013 – Accepted: 27 May 2013 – Published: 27 June 2013

Correspondence to: M. Lupi (matteo.lupi@erdw.ethz.ch)

Published by Copernicus Publications on behalf of the European Geosciences Union.

Abstract

Eruptive rates in volcanic arcs increase significantly after mega-thrust earthquakes in subduction zones. Over short to intermediate time periods the link between mega-thrust earthquakes and arc response can be attributed to dynamic triggering processes or static stress changes, but a fundamental mechanism that controls long-term pulses of volcanic activity after mega-thrust earthquakes has not been proposed yet.

Using geomechanical, geological, and geophysical arguments, we propose that increased eruption rates over longer timescales are due to the relaxation of the compressional regime that accompanies mega-thrust subduction zone earthquakes. More specifically, the reduction of the horizontal stress σ_h promotes the occurrence of short-lived strike-slip kinematics rather than reverse faulting in the volcanic arc. The relaxation of the pre-earthquake compressional regime facilitates magma mobilization by providing a short-circuit pathway to shallow depths by significantly increasing the hydraulic properties of the system. The timescale for the onset of strike-slip faulting depends on the degree of shear stress accumulated in the arc during inter-seismic periods, which in turn is connected to the degree of strain-partitioning at convergent margins.

We performed Coulomb stress transfer analysis to determine the order of magnitude of the stress perturbations in present-day volcanic arcs in response to five actual mega-thrust earthquakes; the 2005 M8.6, 2007 M8.5, and 2007 M7.9 Sumatra earthquakes; the 2010 M8.8 Maule, Chile earthquake; and the 2011 M9.0 Tohoku, Japan earthquake. We find that all, but one, the shallow earthquakes that occurred in the arcs of Sumatra, Chile and Japan show a marked lateral component. Our hypothesis suggests that the long-term response of volcanic arcs to subduction zone mega-thrust earthquakes will be manifested as predominantly strike-slip seismic events, and that these future earthquakes will be followed closely by seismic swarms, inflation, and other indications of a rising magma source.

SED
5, 811–839, 2013

1 Introduction

One of the fundamental uncertainties in earth science is the mechanism controlling volcanism in compressional environments. Horizontally-oriented stresses during compression produce high confining pressures on incipient flow paths, suppressing vertical flow. Instead, this favours sill development when the pressure of magma at depth exceeds the minimum principal stress. Reviews of the structural and petrological characteristics of volcanic systems associated with reverse and strike-slip faults (Tibaldi et al., 2010) show how evolutionary effects of the local stress field affect eruption rates and volcanic behaviours. Over non-geological time periods, the complexity of these systems is due in part to variations in the loading environment throughout mega-thrust earthquake cycles, from sub-horizontal compression during convergence, to short-lived viscoelastic relaxation during post-seismic periods. Indeed, volcanic belts in convergent margins undergo different tectonic regimes that either restrict or promote vertical migration of deep fluids and magmas by the cyclic loading and unloading of the effective normal stress caused by the cyclical occurrence of mega-thrust slips at the subduction interface.

A link between mega-thrust earthquakes and volcanic activity was first recognised by Charles Darwin when he noted increased volcanism in Chile following the M8.5 Conceptión 1835 earthquake (Darwin, 1840). Seismically-induced volcanic activity with varying time- and space-scales is now recognised around the globe (Eggert and Walter, 2009), with examples from the USA (Lipman and Mullineaux, 1981; Sanchez and McNutt, 2004), Kamchatka (Walter, 2007), Central America (Williams and Self, 1983; White and Harlow, 1993), Japan (Koyama, 2002), and Italy (Sharp et al., 1981; Nercessian et al., 1991; Marzocchi et al., 1993; Nostro et al., 1998).

Triggered volcanic activity spans a range of timescales and distances (Hill et al., 2002; Delle Donne et al., 2010). In the immediate or short term associated with passing seismic waves, mechanical perturbation of the magma reservoir can result in processes such as rectified diffusion, gas exolution, and/or unclogging of migration path-

SED
5, 811–839, 2013

ways (i.e. Hill et al., 2002; Manga and Brodsky, 2006; Brodsky and Prejean, 2005). Examples include the Kamchatka M9.0 earthquake in 1952 (Johnson and Satake, 1999), which was followed by eruptions of the Karpinsky and Tao-Rusyr volcanoes one and seven days, respectively, after the main shock (Walter and Amelung, 2007), and the Minchinmavida and Cerro Yanteles volcanoes that erupted less than 24 h after the Conceptión, Chile, earthquake (Darwin, 1840; Cembrano and Lara, 2009).

Static stress changes induced by slip on the subduction interface develop at short to intermediate timescales, principally by relaxing the normal stress that acts on incipient flow pathways (Cembrano and Lara, 2009). The delay between earthquakes and volcanic unrest can extend to years, with some relationship of the hypo-central distance to the volcanic system (Walter and Amelung, 2007). For example, a M8.3 subduction earthquake in 1923 in Kamchatka triggered many subsequent volcanic eruptions in the region, with two in 1923, one in 1925, two in 1926, and one each in 1927, 1928, 1929 and 1930 (Eggert and Walter, 2009). More recent examples include the Planchón-Peteroa, Puyehue-Cordón Caulle, and Copahue volcanoes that erupted approximately seven, sixteen, and thirty-four months after the M8.8 February 2010 Maule earthquake, respectively. The mechanism that drives proposed static stress triggering at intermediate to long timescales remains unclear, but recent studies (Walter and Amelung, 2007; Bonali et al., 2012) suggest that reductions of the effective stress in response to slip along mega-thrust subduction interfaces may contribute to magma mobilization.

In this paper we expand on this concept to explore long-term and evolving changes in the stress state in the arc following mega-thrust subduction zone earthquakes. We propose a mechanism that operates at time-scales greater than the immediate effects of dynamic-stress triggering and long after static stress changes from mega-thrust earthquakes have perturbed the system. We explore the mechanical consequences of a decadal change in the kinematics associated with the post-seismic relaxation and suggest that the tectonic switch from pre-earthquake compression to post-earthquake relaxation results in a dominantly strik-slip stress state emplaced during the "less compressive" time window that follows mega-thrust slips. In this context, increases

SED
5, 811–839, 2013

of crustal permeability via normal stress reduction and strike-slip faulting become the most efficient mechanism for vertical migration of melts and deep slab-derived trapped fluids.

2 Short-lived tectonic switch: proposed mechanism

We hypothesise that long-term increase in arc volcanism is kinematically-controlled whereby post-seismic relaxation of the compressional stress regime initiates short-lived strike-slip kinematics in the volcanic arc. The onset of strike-slip faulting is controlled by (i) the degree of strain partitioning at convergent margins, (ii) the inter-seismic duration that controls the shear stress amplitudes, and (iii) the relative values of the vertical σ_v and horizontal σ_h principal stresses before the mega-thrust earthquake. The onset of strike-slip faulting promotes increases of volcanism because it provides a short-circuit pathway for upwelling fluids and magmas. Strike-slip faulting dramatically increases the vertical permeability of the crustal transport network and may induce high strain rates in the magmatic reservoir if the magmatic chamber is affected by the fault plane (Chaussard and Amelung, 2012). This further promotes the vertical migration of the magma by reducing the effective viscosity of the non-Newtonian melt (Mazzini et al., 2009). Crustal increases of permeability and viscosity drop act in tandem and both promote magma mobilization.

The degree of strain-partitioning strongly affects the switch from reverse to strike-slip environments (Chemenda et al., 2000). In addition, the closer the absolute values of σ_h and σ_v are before the mega-thrust earthquake, the more the switch from reverse to strike-slip faulting is favoured. The mechanical argument is illustrated in the 3-D Mohr-diagram in Fig. 1. In compressive subduction systems, thrust faulting is favoured prior to mega-thrust earthquakes, with the maximum principal stress ($\sigma_1 = \sigma_H$) assumed to be horizontal in the direction of convergence, the minimum principal stress ($\sigma_3 = \sigma_v$) vertical (weight of the overburden), and the intermediate principal stress ($\sigma_2 = \sigma_h$) also horizontal and orthogonal to σ_H. This stress state favours sill development, thrust fault-

SED
5, 811–839, 2013

ing, and inhibits vertical dike formation and propagation (Tibaldi et al., 2010). The maximum shear stress developed during compression is $\tau_{max} = (\sigma_H - \sigma_v)/2$ and it is proportional to the angle of incidence of the ongoing subduction (Chemenda et al., 2000). In this stress state, optimally oriented faults are thrust faults dipping at around 30° assuming a friction coefficient of 0.6. Slip along the mega-thrust interface predominantly relaxes σ_H. Ignoring poro-elastic effects, σ_H and σ_h are coupled, so as σ_H is continuously reduced during the relaxation process, so too is σ_h (albeit at a slower rate). The overburden σ_v remains unchanged, so if σ_h reduces below σ_v the stress state in the arc emerges as a strike-slip regime. The time required to achieve strike-slip faulting depends on the stress difference between σ_h and σ_v prior to the mega-thrust earthquake. For this reason, the switch from reverse to strike-slip regimes is favoured in the arc where σ_v and σ_h are closer (Fig. 1). This implies that, compared to fore- or backarc regions, smaller reductions of σ_h are needed beneath the volcanic arc for σ_v to become the intermediate principal stress.

2.1 Supporting arguments

Geochemical studies in arc lavas suggest transport of slab-derived fluids originated at depth and mobilised over short time scales (e.g. Sigmarsson et al., 1990, 2002). A textbook example that illustrates the mechanism proposed in this paper is provided by the recent evolution of the Laguna del Maule system, which is a volcanic complex located in the fold and thrust belt of Central Chile, facing the main slip of the Maule earthquake. InSAR studies highlight an inflation phase that began in 2007 and reached an average value of 227 mm yr^{-1} in early 2012 (Le Mével et al., 2012). The inflation strongly and suddenly accelerated to 388 mm yr^{-1} after the occurrence of a strike-slip M6.0 earthquake on 17 June 2012, which occurred beneath the volcanic system (Fig. 3).

Strike-slip faulting has been shown to enhance the development of piercement structures in laboratory experiments, with numerical and analogue modelling highlighting that fluid mobilisation is enhanced by shearing-induced reductions in effective viscosity (Mazzini et al., 2009). This is an efficient mobilisation mechanism for non-Newtonian

SED
5, 811–839, 2013

viscous fluids (e.g. magmas) because if the magmatic reservoir is sheared during high strain rate slip events, the concomitant reductions in the effective viscosity make it much more mobile. Although very high strain rates (and therefore very low effective viscosity) are transient, they occur exactly when highly permeable channels are formed during slip. The result is rapid transport over short timescales. Faulting as a mechanism for seismic pumping of deeply trapped fluids has been proposed by Sibson et al. (1975), and contributed to explain aftershock sequences in the Italian Apennines (Miller et al., 2004), or the emplacement of ore deposits (Cox and Ruming, 2004).

Our conceptual model is also consistent with other speculative but yet intriguing examples where magma mobilisation is restricted during thrusting and accelerates significantly once large part of the compressive stress is removed via large-scale slip on the subduction zone interface. For instance, studies of crystal growth (Druitt et al., 2012) show that Santorini volcano, Greece, lay dormant for 18 kyr before evolving into a caldera-forming eruption (ca. 1600 BC) in a mere 100 yr. Driessen and Macdonald (1997) highlights the occurrence of seismically-induced ruins of the Minoan civilisation on the isle of Thera pre-dating the eruption of Santorini. If that earthquake occurred on the Hellenic subduction zone, then it is consistent with our hypothesis where a mega-thrust earthquake transformed the stress state in the arc hosting Santorini into extension or transtension, and initiated the observed rapid magma mobilisation. Another example is the recent eruption of the Chaitén volcano, Chile, that entered a new eruptive phase in May 2008 after more than 9 kyr of dormancy. Wicks et al. (2011) suggest that mobilisation of the viscous rhyolitic magma that fed the eruption was accelerated by the introduction of (mechanically-created) permeability and pressurisation of the magmatic chamber due to the 1960 Valdivia mega-thrust earthquake. Interestingly, a temporary network deployed in 2004 and 2005 around the Chaitén volcano showed clusters of seismicity at the source of that eruption with strike-slip focal mechanisms (Wicks et al., 2011). Finally, Mount Sinabung in Sumatra, after 400 yr of quiescence, erupted in August and September 2010, five years after the 2005 M8.6 Nias earthquake. Sinabung volcano, which resides upon the Great Sumatran strike-slip fault, is located about 180 km East of the region of maximum slip during the Nias earthquake (Hendrasto, 2011).

3 Strain partitioning and observed focal mechanisms in the arc

If strike-slip faulting contributes to magma mobilisation, then it is important to determine to what extent strike-slip faults in the arc were perturbed from slip on subduction interface. Figure 2 shows tectonic settings, slip distributions, and direction of the volcanic arcs for Sumatra, Chile, and Japan. In oblique subduction zones the shear component is accommodated in the overriding plate by trench-parallel, regional-scale, strike-slip faults that are localised within the volcanic belt because of the higher geothermal gradients. Several authors investigated the dynamics of strain partitioning using mathematical (Platt, 1993; Braun and Beaumont, 1995), experimental (Pinet and Cobbold, 1992; Burbidge and Braun, 1998), and field (Rosenau et al., 2006) studies. Fitch (1972) suggests that the strike-slip component relates linearly to the incidence angle of the subduction, with some relation between normal and shear stresses. Chemenda et al. (2000) highlights that the degree of stress partitioning is proportional to the rate of along-trench translation and inversely proportional to the convergence rate and incidence angle. These observations are consistent with the behaviour in the oblique-subducting margins of Chile and Sumatra where strain is partitioned and that showed strike-slip faulting in the arc (Fig. 3). Little partitioning is expected in Japan because of the frontal collision, but some strike-slip faulting following the Tohoku earthquake was observed along the periphery of the perturbed regions, and close to the Itoigawa–Shizuoka and Ishigaki–Kuga tectonic lines, in proximity of mapped reverse faults. This is in agreement with a progressive reduction of σ_h, which promotes σ_v to become the intermediate principal stress. However, fault reactivation and magma mobilization are not always coupled and when this happens (i.e. Laguna del Maule Le Mével et al., 2012) many (unknown) factors (such as crustal permeability, magma viscosity, current

SED
5, 811–839, 2013

stress-state of the volcanic system) may affect the time-delay between faulting and magma mobilization.

4 Coulomb stress transfer to the arc

Coulomb stress transfer is a commonly used tool to determine the change in normal and shear stress on defined planes (receiver faults) due to slip on elastic dislocations in a 3-dimensional half-space (King et al., 1994; Stein, 1999; Toda et al., 2011). We performed Coulomb stress analysis using published slip distributions (USGS, 2010; Ji) as the source faults for the 2005 M8.6, 2007 M8.5, and 2007 M7.9 Sumatra earthquakes; the 2010 M8.8 Maule, Chile earthquake; and the 2011 M9.0 Tohoku, Japan earthquake. As receiver faults we used the strike, dip, and rake angle provided by moment tensor solutions of shallow (less than 20 km deep) strike-slip earthquakes listed in the GMT catalogs that occurred in each of the volcanic arcs following the mega-thrust earthquake. Moment tensor solutions for seismic events weaker than M5 are not always available. Hence, we only account for focal mechanism of events larger than M5. We also acknowledge the sensitivity of Coulomb analyses to the selected parameters. Here we are only concern about the order of magnitude of the stress variations imparted in the arc by the mega-thrust earthquake.

4.1 Sumatra

Oblique convergence in Sumatra is accommodated by trench-normal subduction and trench-parallel transform motion along the Sumatra transform fault. Three mega-thrust subduction zone earthquakes occurred in 2005 and 2007, producing trench-normal slip along most of the island. We do not consider the 2004 M9.2 earthquake because slip from that earthquake occurred primarily to the North of Sumatra where there is no arc. Substantial shear stress along the Sumatran fault is expressed by the occurrence of six M > 5.0 strike-slip faulting events between 2006 and 2009. Figure 4 shows that

SED
5, 811–839, 2013

the regions where these events occurred were mechanically perturbed by the mega-thrust slip either by increase of shear or normal stress. In the first case, seismic or aseismic lateral slip may shear the magmatic reservoir (for instance located upon the Great Sumatran Fault) reducing its effective viscosity by orders of magnitude and thus enhancing its mobility. In the second case, the reduction of normal stress promotes increases of permeability and upwelling of deep fluids that reduce further the effective normal stress bringing faults closer to failure. Additional events with strike-slip focal mechanisms may be predicted in the coming years as post-seismic relaxation of the compressional regime will continue to trigger the transform component of strain-partitioning.

4.2 Chile

The region that faces the slip of the M8.8 2010 Maule earthquake is North of the Liquiñe-Ofqui Transform system, but oblique convergence of the Nazca and South American plates also provides for shear stress development in the thick and old crust North of 37° S. This is shown by two $M > 5$ strike-slip earthquakes that occurred 6 months and 30 months after the Maule earthquake in the fold and thrust belt of Central Chile (Bonali et al., 2012), where lateral motion is not highlighted by mapped strike-slip faults. In the Coulomb analysis of Fig. 5, we choose receiver faults with strike, dip, and rake determined from moment tensor solutions of the M6.0 strike-slip event in the Chilean arc.

The results in Fig. 5 are for the fault plane subparallel to the direction of the arc; results for the antithetic fault plane (striking NW–SE) are discussed later. The stress transfer analysis shows effects of the Maule earthquake, and highlights that fault planes subparallel to the direction of the arc were loaded towards failure. Although much of the Coulomb failure stress is due to the reduction of the normal stress, we also observe a remarkable increase in shear stress. Figure 5 (post-seismic state) shows increased shear and reduced normal stress where observed strike-slip focal mechanisms occurred, indicating that the stress state in the arc is currently accommodating the lateral component.

4.3 Japan

In Japan, strain partitioning is negligible because of the nearly frontal subduction of the Pacific plate beneath the Eurasian plate. This is also confirmed by the reverse focal mechanisms of large magnitude seismic events occurring in the Japanese arc before the 11 March 2011 mega-thrust earthquake (i.e. on 13 June 2008 or 20 September 2010, see Vannucci and Gasperini, 2009, for additional focal mechanisms). The distribution of the volcanic systems in the Japanese arc may also reflect the absence of a through-going strike-slip fault system (Nakamura et al., 1977). The strike-slip focal mechanisms immediately following the Tohoku earthquake are in complicated regions that accommodate the differential (strike-slip) motion of the Pacific and Philippine Plates with respect to the Eurasian plate. Strike-slip seismic events (blue circles of Fig. 3c) occur in regions characterised by thrust faulting (i.e. close to the Kuroiwayama, Furumi, Juchihara, and Zenkoji faults – see AIS, for a complete database of Japanese faults). The reactivation of such systems with strike-slip kinematics can be explained by the short-lived tectonic switch illustrated in Fig. 1. Figure 6 shows a Coulomb stress transfer analysis from slip of the M9.0 2011 Tohoku earthquake (USGS, 2010). As receiver fault we used the plane sub-parallel to the direction of the arc identified by the focal solution of a M5.4 event (11 April 2011). The analysis shows that the entire region was mechanically perturbed and faults were brought closer to failure, consistently with static stress transfer as an earthquake triggering mechanism.

5 Discussion

Sumatra, Central Chile and Japan constitute a spectrum of strain partitioning, and therefore the behaviour of their respective arcs may record this. The Coulomb stress

SED
5, 811–839, 2013

transfer analysis in Sumatra, Chile, and Japan shows that earthquakes with strike-slip focal mechanisms were all brought closer to failure after each of the mega-thrust earthquake. We recognise that stress transfer results are sensitive to many of the input parameters, and the results can change with uncertainties in the slip distribution and/or the orientation or slip of the receiver faults. Nevertheless, the general behaviour of volcanic arcs is consistent with the Coulomb stress transfer picture that emerges. Namely, a strike-slip regime is activated by mega-thrust earthquakes with an apparent correlation between the degree of strain partitioning and the number of strike-slip earthquakes. Although the time window is different between the three systems (with Japan being the most recent event), there have been six large strike-slip events in the Sumatran arc, two in Chile (far from the Liquiñe–Ofqui transform system), and one in the arc directly behind the Tohoku rupture zone (four around the tectonically complex Itoigawa–Shizuoka and Ishigaki–Kuga tectonic lines).

Geological and geophysical observations show that strain partitioning is most pronounced in Sumatra where the high obliquity of convergence between the Australian and Sunda plates results in convergence accommodated by subduction and the strike-slip component taken up by the Great Sumatran Fault. The recent large intra-oceanic plate earthquakes off Sumatra (Duputel et al., 2012) now appear to also take up some strike-slip component, but the existence of the through-going Great Sumatran Fault points to significant shear stress development along the arc. In Central Chile, where a well-developed lateral transport system does not occur, focal mechanisms of recent events confirm that considerable shear stress has developed in the arc (see also Cembrano and Lara, 2009, for additional focal mechanisms).

Focal mechanisms are ambiguous as to which fault plane failed. In Sumatra, the likely true fault plane is subparallel to the strike of the Sumatra Fault, while in Japan there appears to be no visible strike-slip system in the arc behind the Tohoku slip zone. Central Chile, where the Maule earthquake occurred, is interesting because it lies to the North of the through-going Liquiñe–Ofqui Fault, and does not appear to exhibit a regional scale transform system. Tectonic settings controlled by a strong compressional

SED
5, 811–839, 2013

component show a general diffuse distribution of volcanic centres (Nakamura et al., 1977), with a direct correlation between convergence and diffusion of the volcanic systems (Tibaldi et al., 2010). This is consistent with the diffuse distribution of volcanoes on Japan. In Sumatra, volcanic centres are aligned along the Great Sumatra fault, while in South Chile the arc is cut by the Liquiñe–Ofqui transform system. The Liquiñe–Ofqui terminates around 38° S and towards the North the volcanic arc still runs sub-parallel to the subduction zone. However, an accurate analysis shows that Chilean and Argentinean volcanoes may also align along apparent NW–SE oriented lineaments, antithetic to the direction of the arc. Interestingly, these lineaments are sub-parallel to basement NW–SE trending lineaments that have been interpreted as ancient deep structures reactivated as left-lateral strike-slip faults during the development of the volcanic belt (Cembrano and Lara, 2009). Such distribution, which is subparallel to the compressional component of the subduction, recalls the regional-scale lineaments along which italian volcanic systems align (Rosenbaum et al., 2008). Such structures have also being identified in North Fiji, Sulawesi, Indonesia, and at the margins of Calabrian, Caribbean and Scotia arcs (Schellart et al., 2002; Rosenbaum et al., 2008). Cembrano and Lara (2009) highlights that these lineaments can be reactivated by supralithostatic magmatic pressures and our analysis shows that also NW–SE striking faults have been perturbed by mega-thrust earthquakes (Fig. 7).

If the volcanoes in Central Chile are affected by strike-slip motion along NW–SE trending lineaments, then a conjectural mechanism to explain their reactivation is the "bookshelf mechanism" (Mandl, 1987). That is, shear stress develops along strike-slip faults during convergence, but as the compressional stress σ_H is reduced from slip on the subduction zone interface and post-seismic relaxation, deformation is taken up by left-lateral motion along the interfaces of the "books". As stated in Mandl (1987): "*... when the lateral support is relaxed, the books tilt to one side and shift the plank ... The rotation of the books is accompanied by slip between the individual books ...*". Indeed, regions separated by the alignment of Chilean and Argentinean volcanoes resemble tilted books, and faults can be reactivated by slip-induced static stresses.

SED
5, 811–839, 2013

From a deformation standpoint, we have shown that the reactivation of the strike-slip component in volcanic arcs is a common post-seismic response to mega-thrust subduction zone earthquakes. Initiation of strike-slip faulting is started by stress transfer from slip on the subduction interface but post-seismic increasing of crustal hydraulic properties (due to reductions of the normal stress shown in Figs. 4–7) facilitate the development of this mechanism. Permeability is strongly (e.g. exponentially) dependent on the effective normal stress acting on steeply dipping fractures (e.g. Sibson, 1990; Rice, 1992; Miller et al., 2004; Sibson, 2007) and vertical diffusion and advection of fast-migrating deep fluids further decrease the effective normal stress at shallower crustal depths (Sibson, 1992; Cox and Ruming, 2004; Lupi et al., 2011). Our Coulomb study provides a first estimate of the variations of normal and shear stress imposed by the mega-thrust slip and such (few-bars) variations may affect the equilibrium of magmatic plumbing systems by reducing the confining pressure on magmatic reservoirs (Wicks et al., 2011). This can promote the pressurisation of the magmatic chambers by volatile exolution and initiate inflation (Druitt et al., 2012). In addition, co-seismic faulting further increases the permeability of the system by creating new fractures (flow paths) inducing fluid pressure cycles that may causes important changes in physical parameters such as seismic velocities, reflectivity, and electrical conductivity within the seismogenic zone (Sibson, 2009). Such coupled and transient permeability-fluid flow behaviours are thought to be relevant in volcanic and hydrothermal systems, in critically stressed geological environments like subduction zones (e.g Ingebritsen and Sanford, 1999), and may contribute to the formation of gold deposits (Weatherley and Henley, 2013).

Figure 8 summarises the short-lived switch mechanism that we propose to explain the long-term pulse of increased volcanic activity after mega-thrust earthquakes. Namely, the mega-thrust slip reduces the magnitude of the horizontal stress tensors and σ_h becomes smaller than σ_v. If fault-slip includes shearing of the magmatic reservoir, then localised high strain rates decrease the viscosity of the magma encouraging

SED
5, 811–839, 2013

buoyant rise of melts by enhanced buoyancy-driven flow (Connolly and Podladchikov, 2007).

6 Conclusions

We proposed a mechanism to explain the pulsing eruptive rates in volcanic arcs over decades in response to mega-thrust earthquakes. Our hypothesis is based on the enhancement/establishment of strike-slip regimes in the overriding plate of oblique subduction zones after mega-thrust earthquakes. Beneath the volcanic arc, in regions where pre-slip $\sigma_v = \sigma_3$ is close to $\sigma_h = \sigma_2$ the slip-induced reduction of σ_H and σ_h and post-seismic relaxation of compressional stresses results in the vertical stress σ_v adopting the intermediate principal stress. The time-delay between mega-thrust earthquakes and subsequent volcanism reflects the time needed to accommodate the new tectonic loading environment, which depends on the degree of strain-partitioning and shear stress development in the arc. Activation of the (steeply-dipping) strike-slip regime then promotes vertical magma migration by providing a shorter pathway to shallow depths and through faulting-induced increases in the permeability structure. In cases where faulting encompasses the magma chamber itself, then high strain rates during shear additionally favours magma migration from the large-scale reduction in effective viscosity of non-Newtonian magmas. Upwelling of deep fluids increases pore pressure along the flow path, and thus the effective normal stress acting on steeply dipping fractures and faults reduces even further, initiating a feedback of fracture, flow, and volatile exsolution.

Coulomb stress transfer analyses in Sumatra, Japan, and Chile all show that strike-slip faults that failed less than 10 yr after the mega-thrust earthquake were brought closer to failure by the main event. Future studies and observations should focus on strike-slip events expected to occur in theses volcanic arcs, with efforts in Central Chile to determine which of the ambiguous focal mechanism solutions is the true fault plane and which is the auxiliary fault plane. We also expect that strike-slip faulting in the arcs of Chile and Sumatra will be followed closely by indicators of a rising magma source, including swarms, inflation, and eruptions. Our hypothesis can be tested in a way that includes (i) structural studies of volcanic arcs to confirm the coexistence of strike-slip and reverse faulting regimes; and (ii) seismic, geodetic, and geochemical networks to capture the expected behaviour described in this paper.

Acknowledgements. The authors thank the Humanitus Sidoarjo fund for partially support this study. Discussions with N. Mancktelow and G. L. Cardello are highly appreciated. J. P. Burg and M. Frehner are thanked for commenting the manuscript and improving its status.

References

AIST, available at: http://riodb02.ibase.aist.go.jp/activefault/index_e.html, Active fault database of Japan; Last Access date: 13th of June 2013; Year of Publication (of the English Version) 1st of December 2005. 821

Bonali, F., Tibaldi, A., Corazzato, C., Tormey, D., and Lara, L.: Quantifying the effect of large earthquakes in promoting eruptions due to stress changes on magma pathway: the Chile case, Tectonophysics, 583, 54–67, doi:10.1016/j.tecto.2012.10.025, 2012. 814, 820

Braun, J. and Beaumont, C.: Three-dimensional numerical experiments of strain partitioning at oblique plate boundaries: Implications for contrasting tectonic styles in the southern Coast Ranges, California, and central South Island, New Zealand, J. Geophys. Res., 100, 18059–18074, 1995. 818

Briggs, R. W., Sieh, K., Meltzner, A. J., Natawidjaja, D., Galetzka, J., Suwargadi, B., Hsu, Y.-J., Simons, M., Hananto, N., Suprihanto, I., Prayudi, D., Avouac, J. P., Prawirodirdjo, L., and Bock, Y.: Deformation and slip along the Sunda megathrust in the great 2005 Nias–Simeulue earthquake, Science, 311, 1897–1901, 2006. 833

Brodsky, E. E. and Prejean, S. G.: New constraints on mechanisms of remotely triggered seismicity at Long Valley Caldera, J. Geophys. Res.-Sol. Ea., 110, B04302, doi:10.1029/2004JB003211, 2005. 814

Burbidge, D. R. and Braun, J.: Analogue models of obliquely convergent continental plate boundaries, J. Geophys. Res., 103, 15221–15237, 1998. 818

Cembrano, J. and Lara, L.: The link between volcanism and tectonics in the southern volcanic zone of the Chilean Andes: a review, Tectonophysics, 471, 96–113, 2009. 814, 822, 823
Chaussard, E. and Amelung, F.: Precursory inflation of shallow magma reservoirs at west Sunda volcanoes detected by InSAR, Geophys. Res. Lett., 39, L21311, doi:10.1029/2012GL053817, 2012. 815
Chemenda, A., Lallemand, S., and Bokun, A.: Strain partitioning and interplate friction in oblique subduction zones – constraints provided by experimental modeling, J. Geophys. Res., 105, 5567–5581, 2000. 815, 816, 818
Connolly, J. and Podladchikov, Y.: Decompaction weakening and channeling instability in ductile porous media: implications for asthenospheric melt segregation, J. Geophys. Res., 112, B10205, doi:10.1029/2005JB004213, 2007. 825
Cox, S. and Ruming, K.: The St Ives mesothermal gold system, Western Australia – a case of golden aftershocks?, J. Struct. Geol., 26, 1109–1125, 2004. 817, 824
Darwin, C.: On the connexion of certain volcanic phenomena in South America; and on the formation of mountain chains and volcanoes, as the effect of the same power by which continents are elevated, Trans. Geol. Soc. Lond. 5, (2nd ser.), 601–631, 1840. 813, 814
Delle Donne, D., Harris, A. J., Ripepe, M., and Wright, R.: Earthquake-induced thermal anomalies at active volcanoes, Geology, 38, 771–774, 2010. 813
Driessen, J. and Macdonald, C.: The troubled island: Minoan Crete before and after the Santorini eruption (Aegaeum 17), Liège and Austin, Aegaeum, 1997. 817
Druitt, T., Costa, F., Deloule, E., Dungan, M., and Scaillet, B.: Decadal to monthly timescales of magma transfer and reservoir growth at a caldera volcano, Nature, 482, 77–80, 2012. 817, 824
Duputel, Z., Kanamori, H., Tsai, V. C., Rivera, L., Meng, L., Ampuero, J.-P., and Stock, J. M.: The 2012 Sumatra great earthquake sequence, Earth Planet. Sc. Lett., 351, 247–257, 2012. 822
Eggert, S. and Walter, T.: Volcanic activity before and after large tectonic earthquakes: observations and statistical significance, Tectonophysics, 471, 14–26, 2009. 813, 814
EMSC – Online catalogue, available at: http://www.emsc-csem.org/Earthquake/tensors.php, last access: 13th of June 2013. 834
Fitch, T.: Plate convergence, transcurrent faults, and internal deformation adjacent to southeast Asia and the western Pacific, J. Geophys. Res., 77, 4432–4460, 1972. 818

SED
5, 811–839, 2013

Hendrasto, M.: Learn from 2010 Eruptions at Merapi and Sinabung Volcanoes in Indonesia, Annuals of Disas. Prev. Res., 54, 185–194, 2011. 818

Hill, D., Pollitz, F., and Newhall, C.: Earthquake–volcano interactions, Phys. Today, 55, 41–47, 2002. 813, 814

Ingebritsen, S. and Sanford, W.: Groundwater in Geologic Processes, Cambridge University Press, USA, 1999. 824

Ji, C.: Large Earthquake Database, available at: http://www.geol.ucsb.edu/faculty/ji/big_earthquakes/home.html, last access: 13th of June 2013. 819, 835

Johnson, J. and Satake, K.: Asperity distribution of the 1952 great Kamchatka earthquake and its relation to future earthquake potential in Kamchatka, Pure Appl. Geophys., 154, 541–553, 1999. 814

King, G. C., Stein, R. S., and Lin, J.: Static stress changes and the triggering of earthquakes, B. Seismol. Soc. Am., 84, 935–953, 1994. 819

Koyama, M.: Mechanical coupling between volcanic unrests and large earthquakes: a review of examples and mechanisms, J. Geogr., 111, 222–232, 2002. 813

Le Mével, H., Feigl, K., Tabrez, A., Cordova, L., DeMets, C., and Singer, B. S.: Rapid uplift during the 2007–2012 at Laguna del Maule volcanic field, Andean Southern volcanic zone, AGU Fall Meeting 2012: Poster V31B-2786, San Francisco, California, 3rd to 7th of December 2012, 2012. 816, 818

Lipman, P. and Mullineaux, D.: The 1980 eruptions of Mount St. Helens, Washington, US Dept. of the Interior, US Geological Survey, United States Government Printing Office, Washington, D.C., 1981. 813

Lupi, M., Geiger, S., and Graham, C.: Numerical simulations of seismicity-induced fluid flow in the Tjörnes Fracture Zone, Iceland, J. Geophys. Res., 116, B07101, doi:10.1029/2010JB007732, 2011. 824

Mandl, G.: Tectonic deformation by rotating parallel faults: the "bookshelf" mechanism, Tectonophysics, 141, 277–316, 1987. 823

Manga, M. and Brodsky, E.: Seismic triggering of eruptions in the far field: volcanoes and geysers, Annu. Rev. Earth Pl. Sc., 34, 263–291, 2006. 814

Marzocchi, W., Scandone, R., and Mulargia, F.: The tectonic setting of Mount Vesuvius and the correlation between its eruptions and the earthquakes of the Southern Apennines, J. Volcanol. Geotherm. Res., 58, 27–41, 1993. 813

SED
5, 811–839, 2013

Mazzini, A., Nermoen, A., Krotkiewski, M., Podladchikov, Y., Planke, S., and Svensen, H.: Strike-slip faulting as a trigger mechanism for overpressure release through piercement structures, implications for the Lusi mud volcano, Indonesia, Mar. Petrol. Geol., 26, 1751–1765, 2009. 815, 816
Miller, S., Collettini, C., Chiaraluce, L., Cocco, M., Barchi, M., and Kaus, B.: Aftershocks driven by a high-pressure CO_2 source at depth, Nature, 427, 724–727, 2004. 817, 824
Moreno, M., Rosenau, M., and Oncken, O.: 2010 Maule earthquake slip correlates with pre-seismic locking of Andean subduction zone, Nature, 467, 198–202, 2010. 833
Nakamura, K., Jacob, K. H., and Davies, J. N.: Volcanoes as possible indicators of tectonic stress orientation – Aleutians and Alaska, Pure Appl. Geophys., 115, 87–112, 1977. 821, 823
Nercessian, A., Hirn, A., and Sapin, M.: A correlation between earthquakes and eruptive phases at Mt Etna: an example and past occurrences, Geophys. J. Int., 105, 131–138, 1991. 813
Nostro, C., Stein, R., Cocco, M., Belardinelli, M., and Marzocchi, W.: Two-way coupling between Vesuvius eruptions and southern Apennine earthquakes, Italy, by elastic stress transfer, J. Geophys. Res., 103, 24487–24504, 1998. 813
Ozawa, S., Nishimura, T., Suito, H., Kobayashi, T., Tobita, M., and Imakiire, T.: Coseismic and postseismic slip of the 2011 magnitude-9 Tohoku–Oki earthquake, Nature, 475, 373–376, 2011. 833
Pinet, N. and Cobbold, P.: Experimental insights into the partitioning of motion within zones of oblique subduction, Tectonophysics, 206, 371–388, 1992. 818
Platt, J.: Mechanics of oblique convergence, J. Geophys. Res., 98, 16–239, 1993. 818
Rice, J. R.: Fault stress states, pore pressure distributions, and the weakness of the San Andreas Fault, in Fault Mechanics and Transport Properties in Rocks: A Festschrifi in Honor of W. F. Brace, edited by: Evans, B. and Wong, T.-F., Academic Press, London, ISBN 0122437802, 1992. 824
Rosenau, M., Melnick, D., and Echtler, H.: Kinematic constraints on intra-arc shear and strain partitioning in the southern Andes between 38 S and 42 S latitude, Tectonics, 25, TC4013, doi:10.1029/2005TC001943, 2006. 818
Rosenbaum, G., Gasparon, M., Lucente, F. P., Peccerillo, A., and Miller, M. S.: Kinematics of slab tear faults during subduction segmentation and implications for Italian magmatism, Tectonics, 27, TC2008, doi:10.1029/2007TC002143, 2008. 823

SED
5, 811–839, 2013

Sanchez, J. and McNutt, S.: Intermediate-term declines in seismicity at Mt. Wrangell and Mt. Veniaminof volcanoes, Alaska, following the 3 November 2002 Mw 7.9 Denali Fault earthquake, B. Seismol. Soc. Am., 94, 6B, S370–S383, doi:10.1785/0120040602004, 2004. 813

Schellart, W., Lister, G., and Jessell, M.: Analogue modeling of arc and backarc deformation in the New Hebrides arc and North Fiji Basin, Geology, 30, 311–314, 2002. 823

Sharp, A., Lombardo, G., and Davis, P.: Correlation between eruptions of Mount Etna, Sicily, and regional earthquakes as seen in historical records from AD 1582, Geophys. J. Roy. Astr. S., 65, 507–523, 1981. 813

Sibson, R.: Conditions for fault-valve behaviour, Geol. Soc. Spec. Publ., 54, 15–28, 1990. 824

Sibson, R.: Implications of fault-valve behaviour for rupture nucleation and recurrence, Tectonophysics, 211, 283–293, 1992. 824

Sibson, R.: An episode of fault-valve behaviour during compressional inversion? – The 2004 MJ 6.8 Mid-Niigata prefecture, Japan, earthquake sequence, Earth Planet. Sc. Lett., 257, 188–199, 2007. 824

Sibson, R.: Rupturing in overpressured crust during compressional inversion – the case from NE Honshu, Japan, Tectonophysics, 473, 404–416, 2009. 824

Sibson, R., Moore, J. M. M., and Rankin, A.: Seismic pumping: a hydrothermal fluid transport mechanism, J. Geol. Soc. London, 131, 653–659, 1975. 817

Sigmarsson, O., Condomines, M., Morris, J., and Harmon, R.: Uranium and 10Be enrichments by fluids in Andean arc magmas, Nature, 346, 163–165, doi:10.1038/346163a0, 1990. 816

Sigmarsson, O., Chmeleff, J., Morris, J., and Lopez-Escobar, L.: Origin of 226Ra–230Th disequilibria in arc lavas from southern Chile and implications for magma transfer time, Earth Planet. Sc. Lett., 196, 189–196, 2002. 816

Stein, R.: The role of stress transfer in earthquake occurrence, Nature, 402, 605–609, 1999. 819

Tibaldi, A., Pasquarè, F., and Tormey, D.: Volcanism in reverse and strike-slip fault settings, in: New Frontiers in Integrated Solid Earth Sciences, 315–348, doi:10.1007/978-90-481-2737-5, SpringerVerlag, Dordrecht, The Netherlands, 2010. 813, 816, 823

Toda, S., Stein, R., Sevilgen, V., and Lin, J.: Coulomb 3. 3 Graphic-rich deformation and stress-change software for earthquake, tectonic, and volcano research and teaching-user guide, Tech. rep., USGS, 2011. 819

SED
5, 811–839, 2013

Tectonic switch after mega-thrust earthquakes

M. Lupi and S. A. Miller

USGS: USGS online archive of significant earthquakes, Tech. rep., available at: http://earthquake.usgs.gov/earthquakes/eqinthenews/, USGS, last access: 13th of June 2013, 2010. 819, 821, 833, 836
Vannucci, G. and Gasperini, P.: The new release of the database of Earthquake Mechanisms of the Mediterranean Area (EMMA Version 2), Ann. Geophys.-Italy, 47, 307–334, 2009. 821
Walter, T.: How a tectonic earthquake may wake up volcanoes: stress transfer during the 1996 earthquake-eruption sequence at the Karymsky volcanic group, Kamchatka, Earth Planet. Sc. Lett., 264, 347–359, 2007. 813
Walter, T. and Amelung, F.: Volcanic eruptions following M 9 megathrust earthquakes: implications for the Sumatra-Andaman volcanoes, Geology, 35, 539–542, doi:10.1130/G23429A.1, 2007. 814
Weatherley, D. K. and Henley, R. W.: Flash vaporization during earthquakes evidenced by gold deposits, Nat. Geosci., 6, 294–298, doi:10.1038/ngeo1759, 2013. 824
White, R. and Harlow, D.: Destructive upper-crustal earthquakes of Central America since 1900, B. Seismol. Soc. Am., 83, 1115–1142, 1993. 813
Wicks, C., de La Llera, J., Lara, L., and Lowenstern, J.: The role of dyking and fault control in the rapid onset of eruption at Chaitén volcano, Chile, Nature, 478, 374–377, 2011. 817, 824
Williams, S. and Self, S.: The October 1902 plinian eruption of Santa Maria Volcano, Guatemala, J. Volcanol. Geotherm. Res., 16, 33–56, 1983. 813

SED
5, 811–839, 2013

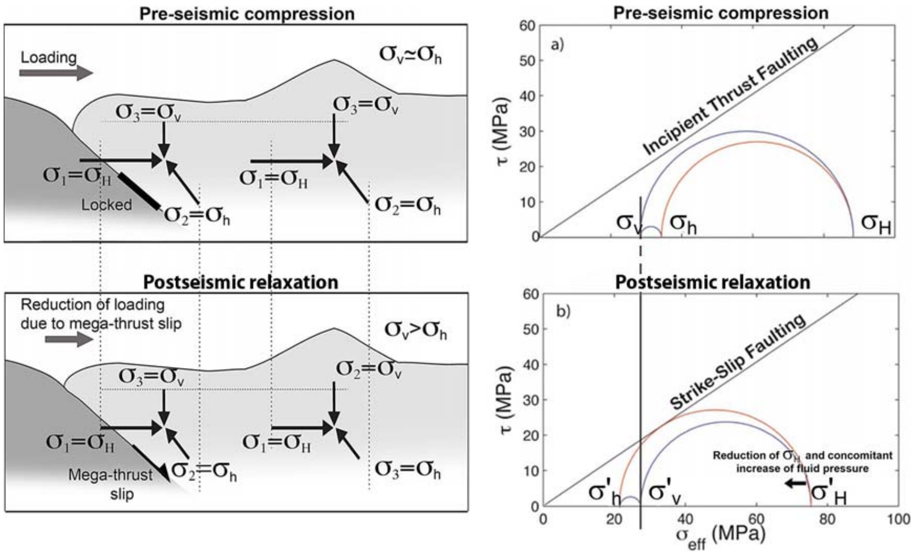

Fig. 1. Mechanical argument for a long-term increase in volcanism following mega-thrust earthquakes. The stress state during compression (loading) encourages thrust faulting, sill development, and limited vertical fluid flow. Beneath the arc, the value of σ_v is higher (and close to σ_h) than at same depths in the fore-arc region. Post-seismic unloading reduces the maximum horizontal stress, while simultaneously increasing vertical permeability (increasing fluid pressure) due to the reduction in fault normal stress. Due to the reduction of σ_H and moreover σ_h, σ_v becomes the intermediate principal stress. This initiates strike-slip faulting in the arc, which coupled with the concomitant increase in hydraulic properties of the flow network, facilitates magma mobilisation.

SED
5, 811–839, 2013

Tectonic switch after mega-thrust earthquakes

M. Lupi and S. A. Miller

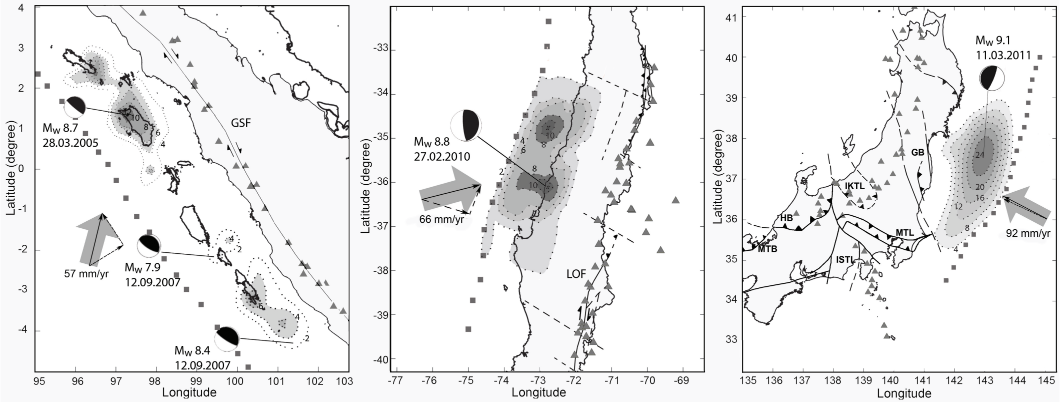

Fig. 2. Tectonic setting and co-seismic slip of the Sumatran, Chilean, and Japanese earthquakes. The M8.7 Nias earthquake occurred on 28 March 2005 at the interface between the Sunda and Australian plates. The maximum slip was calculated to be approximately 14 m (30 km deep) with a rupture plane striking N°35W and dipping 15°, which propagated laterally for approximately 400 km NW–SE and for more than 180 km down-dip (Briggs et al., 2006; USGS, 2010). The M8.5 and M7.9 Sumatran earthquakes occurred on 12 September 2007 and caused maximum slips of four and seven metres, respectively. The M8.8 Maule earthquake hit Chile on 27 February 2010 rupturing the Concepción–Constitucion gap at the interface of the Nazca and South America plates. The slip plane (18° NE, 18° S dip) ruptured for more than 100 km downdip and extended approximately 500 km in the north-south direction (USGS, 2010) inducing a maximum slip of 14 m at 35 km depth (Moreno et al., 2010). The M9.0 Tohoku earthquake hit Japan on 11 March 2011, close to the north-east coast of Honshu, Japan where the Pacific plate subduces beneath the North America plate. The slip plane (striking S°19E and dipping is 14° WNW) propagated 400 km along strike and 150 km in the dip direction with a maximum slip of 24 m according to Ozawa et al. (2011). GSF and LOF stand for Great Sumatran Fault and Liquiñe–Ofqui Fault system, respectively. ISTL stands for Itoigawa–Shizuoka tectonic line, MTL for median tectonic line, IKTL for Ishigaki–Kuga Tectonic Line, MTB for Mino–Tanba belt, GB for Gosaisho belt, HB for Hida belt

SED
5, 811–839, 2013

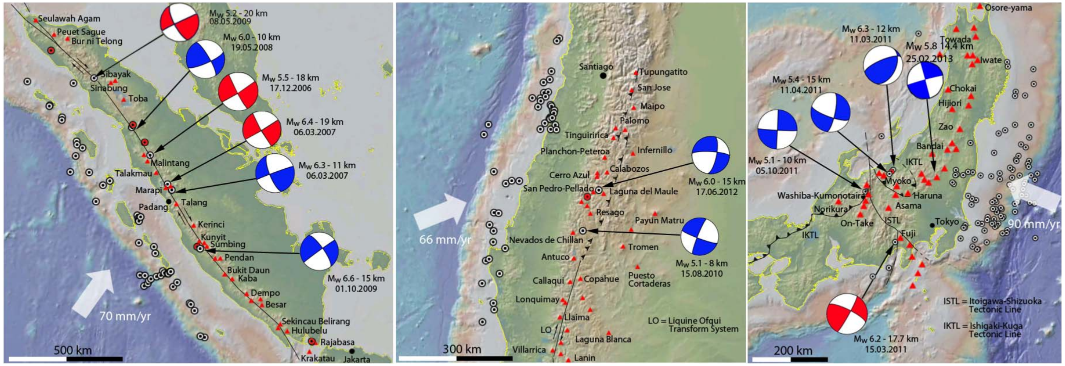

Fig. 3. Maps of Sumatra, Chile, and Japan showing locations of shallow aftershock events that followed the mega-thrust events of Sumatra (M8.7, M8.4, M7.9), Maule (M8.8), and Tohoku (M9.0). Blue focal mechanisms identify seismic events with focus depths shallower than 15 km whereas red focal mechanisms show events deeper than 15 km but shallower than 20 km. The depth-range was selected to identify crustal events only (i.e. relevant to brittle deformation of the arc). Focal mechanisms of seismic events with magnitudes smaller than M5 were not always available from USGS, ESMC, and GMT on-line catalogues and were therefore not plotted to avoid biased estimates of ongoing crustal deformation. White and black-cored circles indicate aftershock activity M > M5 at the subduction interface while red and black-cored circles indicate seismic events (M > M5) in the arc for which focal mechanisms are not available. All the focal mechanism plotted here can be retrieved from catalogue.

SED
5, 811–839, 2013

Tectonic switch after mega-thrust earthquakes

M. Lupi and S. A. Miller

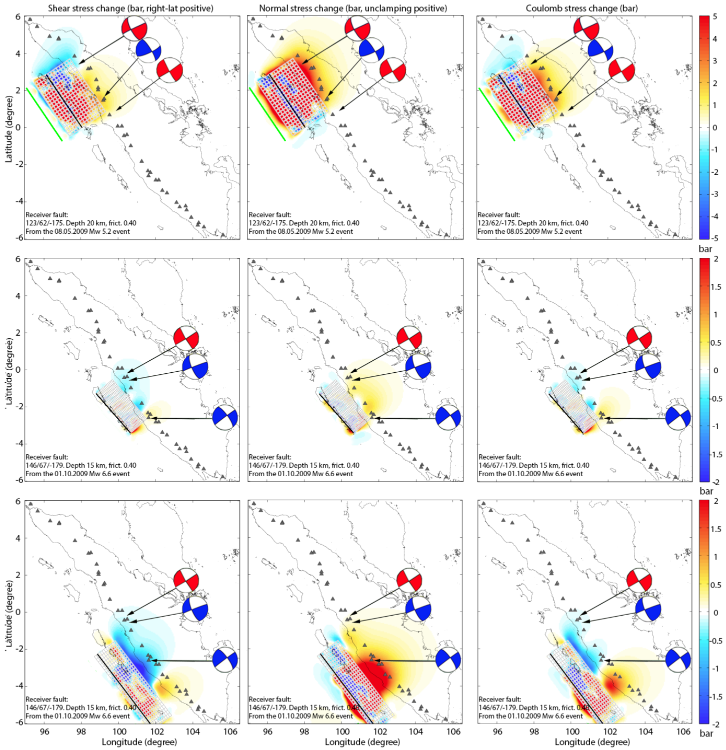

Fig. 4. Coulomb stress analysis for Sumatra. The slip distributions of the events were downloaded from Ji. The first row highlights stress shear, normal, and coulomb stress induced by the 2005 earthquake while the second and third rows indicate effects of the M7.9 and M8.5 2007 earthquakes, respectively. The receiver fault for the Northernmost mega-thrust slip (Nias earthquake) is taken from the fault plane solution of the Mw 5.2 event occurred on 8 May 2009. Depth of the event and strike, dip, and rake angles are shown in each box. For the M7.9 and M8.5 mega-thrust earthquakes we selected the fault plane solution identified by the M6.6 event that occurred on 1 October 2009.

SED
5, 811–839, 2013

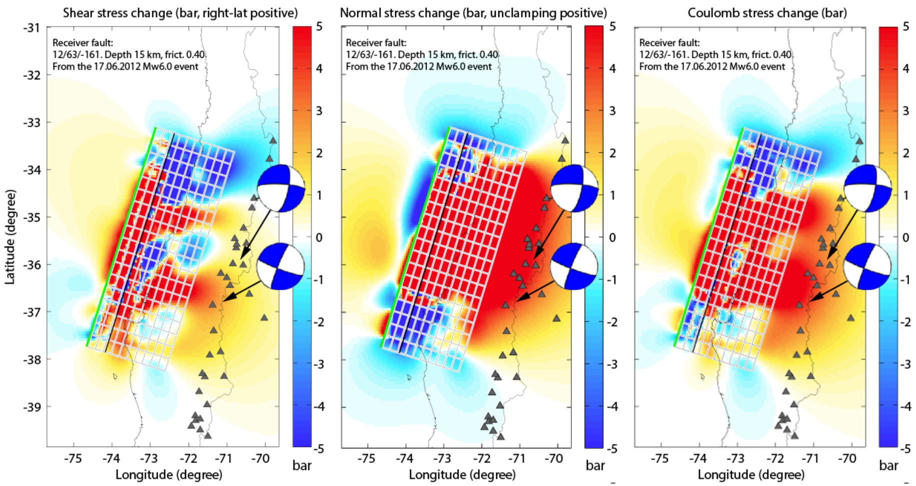

Fig. 5. Shear, normal, and Coulomb stress analysis for Chile. The slip distributions of the Maule earthquake was downloaded from USGS (2010). The receiver fault, subparallel to the strike of the volcanic arc, is taken from the fault plane solution of the Mw 6.0 event occurred on 17 June 2012. Depth of the event and strike, dip, and rake angles are shown the boxes.

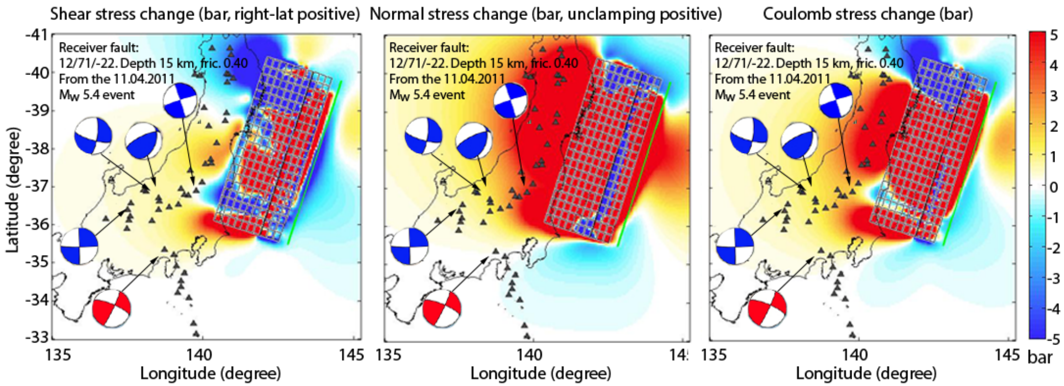

Fig. 6. Coulomb failure calculations of shear, normal, and Coulomb stress induced by the Tohoku–Honsh earthquake on fault plane solutions subparallel to the strike of the volcanic arc. The receiver fault is identified by the focal mechanisms of the M5.4 event in the arc occurred on 11 April 2011.

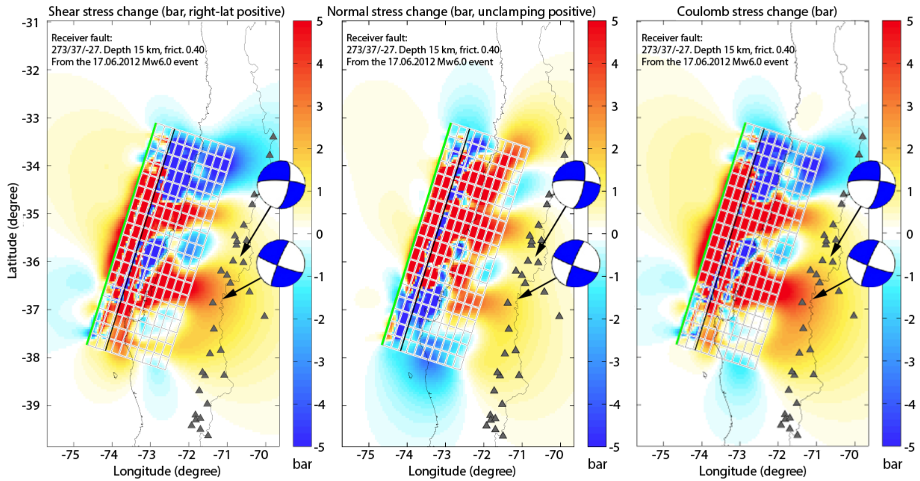

Fig. 7. Shear, normal, and Coulomb stress analysis for Chile using the other fault plane solution of the Mw 6.0 event occurred on 17 June 2012 (antithetic to the direction of the volcanic arc). Depth of the event and strike, dip, and rake angles are shown the boxes. The Coulomb analysis shows that results similar to the ones of Fig. 5are obtained when using alternative fault planes highlighting that the Maule earthquake may have perturbed also ancient fault striking approximately N270.

SED
5, 811–839, 2013

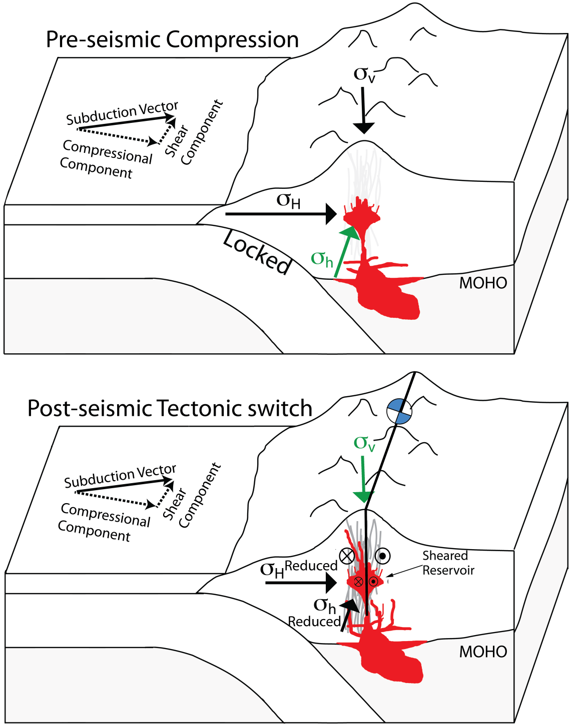

Fig. 8. Simplified representation of the short-lived tectonic switch that takes place in the arc after mega-thrust earthquakes. The green arrow indicates σ_2 and changes from the pre-seismic to the post-seismic state due to the reduction of σ_h as described in Fig. 1. It has to be noticed that while σ_H and σ_h reduce, σ_v remains unchanged. The cartoon also highlights the increase of crustal permeability due to lateral motion (darker grey lines) and the shearing of the non-newtonian body.

SED
5, 811–839, 2013

M. Lupi and S. A. Miller